Frontiers of Information Technology & Electronic Engineering
www.jzus.zju.edu.cn; engineering.cae.cn; www.springerlink.com
ISSN 2095-9184 (print); ISSN 2095-9230 (online)
E-mail: jzus@zju.edu.cn

Multi-UAV obstacle avoidance control via multi-objective social learning pigeon-inspired optimization*

Wan-ying RUAN[1], Hai-bin DUAN[‡1,2]
[1]State Key Laboratory of Virtual Reality Technology and Systems, School of Automation Science and Electrical Engineering, Beihang University, Beijing 100083, China
[2]Peng Cheng Laboratory, Shenzhen 518000, China
E-mail: wyruan@buaa.edu.cn; hbduan@buaa.edu.cn

Received Feb. 10, 2020; Revision accepted Mar. 30, 2020; Crosschecked Apr. 13, 2020

Abstract: We propose multi-objective social learning pigeon-inspired optimization (MSLPIO) and apply it to obstacle avoidance for unmanned aerial vehicle (UAV) formation. In the algorithm, each pigeon learns from the better pigeon but not necessarily the global best one in the update process. A social learning factor is added to the map and compass operator and the landmark operator. In addition, a dimension-dependent parameter setting method is adopted to improve the blindness of parameter setting. We simulate the flight process of five UAVs in a complex obstacle environment. Results verify the effectiveness of the proposed method. MSLPIO has better convergence performance compared with the improved multi-objective pigeon-inspired optimization and the improved non-dominated sorting genetic algorithm.

Key words: Unmanned aerial vehicle (UAV); Obstacle avoidance; Pigeon-inspired optimization; Multi-objective social learning pigeon-inspired optimization (MSLPIO)
https://doi.org/10.1631/FITEE.2000066 **CLC number:** TP242.6; V279

1 Introduction

In recent years, artificial intelligence technologies have rapidly developed, and unmanned systems have been successfully applied in many fields (Floreano and Wood, 2015; Zhang et al., 2017). As part of the unmanned systems, unmanned aerial vehicles (UAVs) play an important role in civil and military fields. In many cases, a UAV cannot accomplish complex tasks that require multi-UAV flocking. Flocking behavior is widespread in nature. Birds flying in groups in the air, creatures moving in groups on the ground, and fish groups under the water are examples of such behaviors. Researchers analyzed swarm behaviors and applied a swarm mechanism to other fields (Biro et al., 2016; Forestiero, 2017; Sun and Turkoglu, 2017; Wang et al., 2017; Yan et al., 2017; Guo et al., 2018). UAV flocking technology is currently a hot issue, but it involves many problems such as cooperative formation flight, formation reconfiguration, and flocking obstacle avoidance (Mohanty and Parhi, 2012; Faisal et al., 2013; Di et al., 2015; Ho and Do, 2017; Kownacki and Ambroziak, 2017; Qiu and Duan, 2017a; Ferri et al., 2018; Benjamin et al., 2019; Molinos et al., 2019). Therefore, multi-UAV obstacle avoidance is a meaningful research subject.

There is a lot of research on obstacle avoidance in UAVs. Based on the Olfati-Saber multi-agent obstacle avoidance framework, a new flocking obstacle avoidance algorithm was proposed, which improves

‡ Corresponding author

* Project supported by the Science and Technology Innovation 2030-Key Project of "New Generation Artificial Intelligence," China (No. 018AAA0102303), the National Natural Science Foundation of China (Nos. 91948204, 91648205, U1913602, and U19B2033), and the Aeronautical Foundation of China (No. 20185851022)

ORCID: Wan-ying RUAN, https://orcid.org/0000-0002-1482-257X; Hai-bin DUAN, https://orcid.org/0000-0002-4926-3202

the cooperative obstacle avoidance capability of UAV flocking (Zhao et al., 2019). A formation control method using local interaction information was implemented, and the effectiveness of the algorithm was verified by flocking simulation through obstacles (Alonso-Mora et al., 2016). Our team has been working on this issue as well. A pigeon hierarchy characteristic was applied to UAV flocking, and a UAV distributed control framework was presented, which shows a stable performance (Luo and Duan, 2017). Considering a pigeon mode of transformation between hierarchical and egalitarian interactions, a pigeon flocking model and a pigeon-coordinated obstacle avoidance model were proposed (Qiu and Duan, 2017b).

Parameter optimization is essential in making the flocking control algorithm perform well. As a new swarm intelligence optimization algorithm, pigeon-inspired optimization (PIO) has shown great potential. Since it was proposed by Duan and Qiao (2014), it has drawn close attention and has been widely used. The multi-objective optimization problem is one of the important applications of PIO. The UAV flocking problem among obstacles was transferred to a multi-objective optimization problem, and an improved multi-objective pigeon-inspired optimization (MPIO) was put forward, realizing that UAVs can fly stably in an obstacle environment (Qiu and Duan, 2020). On this basis, we design a flocking control strategy, propose multi-objective social learning pigeon-inspired optimization (MSLPIO), and realize smooth passage of multiple UAVs among complex obstacles. The social learning mechanism is inspired by the social learning particle swarm optimization (SL-PSO) proposed by Cheng and Jin (2015). They improved particle swarm optimization (PSO) using a social learning mechanism to make the algorithm converge faster. In this study, a social learning mechanism is introduced to MPIO, which improves the convergence of the algorithm and the blindness of parameter setting.

2 Problem formulation

2.1 Unmanned aerial vehicle model

A UAV model is simplified as the first-order Mach number maintaining autopilot, the first-order course maintaining autopilot, and the second-order altitude maintaining autopilot (Wu, 2013; Qiu and Duan, 2020). The specific model is expressed as follows:

$$\begin{cases} \dot{X}_i = V_i \cos\varphi_i, \\ \dot{Y}_i = V_i \sin\varphi_i, \\ \dot{H}_i = \eta_i, \\ \dot{V}_i = -\dfrac{1}{\tau_V}(V_i - V_\text{c}^i), \\ \dot{\varphi}_i = -\dfrac{1}{\tau_\varphi}(\varphi_i - \varphi_\text{c}^i), \\ \dot{\eta}_i = -\left(\dfrac{1}{\tau_\text{a}} + \dfrac{1}{\tau_\text{b}}\right)\eta_i - \dfrac{1}{\tau_\text{a}\tau_\text{b}} H_i + \dfrac{1}{\tau_\text{a}\tau_\text{b}} H_\text{c}^i, \end{cases} \tag{1}$$

where X_i, Y_i, and H_i are the positions of the i^th UAV in the X, Y, and Z directions respectively, V_i, φ_i, and η_i are the horizontal velocity, the horizontal course, and the rate of change in altitude respectively, and τ_V, τ_φ, τ_a, and τ_b are the time constants. V_c^i, φ_c^i, and H_c^i are the inputs of the autopilot for the i^th UAV, and they are expressed as follows:

$$\begin{cases} V_\text{c}^i = \tau_V (u_i^1 \cos\varphi_i + u_i^2 \sin\varphi_i) + V_i, \\ \varphi_\text{c}^i = \dfrac{\tau_V}{V_i}(u_i^2 \cos\varphi_i - u_i^1 \sin\varphi_i) + \varphi_i, \\ H_\text{c}^i = H_i + (\tau_\text{a} + \tau_\text{b})\eta_i + \tau_\text{a}\tau_\text{b} u_i^3, \end{cases} \tag{2}$$

where u_i^1, u_i^2, and u_i^3 denote the control components in the x, y, and z directions, respectively. In addition, the following constraints need to be met:

$$\begin{cases} V_\text{min} \le V_i \le V_\text{max}, \\ |\dot{\varphi}_i| \le \dfrac{n_\text{max} g}{V_i}, \\ \eta_\text{min} \le \eta_i \le \eta_\text{max}, \end{cases} \tag{3}$$

where n_max is the maximum lateral overload and g the gravitational acceleration set to 10 m/s^2.

2.2 Flocking control strategy

During the process of UAV flocking obstacle avoidance, the following movement rules should be ensured: (1) A safe distance should be maintained among UAVs; (2) All UAVs should maintain the same speed; (3) All UAVs should be kept at a desired height; (4) Collision should be avoided between an obstacle and a UAV.

Therefore, we design the flocking control model to include the following components: formation control component, collision avoidance control components among UAVs, obstacle avoidance control component between a UAV and an obstacle, consistent UAV speed control component, expected speed control component, and vertical height control component. Details are as follows (Qiu and Duan, 2020):

$$u_i^k=\begin{cases}u_\mathrm{f}+u_\mathrm{c}+u_\mathrm{o}+u_\mathrm{nv},\ k=1,2,\\ u_\mathrm{ev}+u_\mathrm{eh},\ k=3,\end{cases}\tag{4}$$

where u_i^k represents the total control quantity with k=1, 2, and 3 denoting the corresponding components in the x, y, and z directions, respectively. The components are given in the following.

1. Formation control component u_f:

$$u_\mathrm{f}=C_\mathrm{f}\sum_{j\in\{d_{ij}\le D_\mathrm{c}\}}\alpha(P_j^k-P_i^k)\ln\left(d_{ij}/D_\mathrm{d}\right),\tag{5}$$

where C_f is the formation control coefficient, which is set to 0.2, $d_{ij}=\sqrt{\sum_{k=1}^{2}(P_i^k-P_j^k)^2}$ the horizontal distance between the i^th and j^th UAVs, D_c the communication distance, which is set to 10 m, α the weight factor, P_i and P_j the positions of the i^th and j^th UAVs respectively, and D_d the desired horizontal distance among UAVs, which is set to 10 m.

2. Collision avoidance control component u_c:

$$u_\mathrm{c}=C_\mathrm{c}\sum_{j\in\{d_{ij}\le D_\mathrm{s}\}}\left(\frac{1}{d_{ij}}-\frac{1}{D_\mathrm{s}}\right)^2\frac{P_i^k-P_j^k}{|P_i^k-P_j^k|},\tag{6}$$

where C_c is the collision control coefficient among UAVs, which is set to 10^5, D_s the minimum distance against collision among UAVs, which is set to 2 m.

3. Obstacle avoidance control component u_o:

$$u_\mathrm{o}=\begin{cases}C_\mathrm{o}\alpha(V_\mathrm{e}\cos\delta-v_i^k),\quad k=1,\\ C_\mathrm{o}\alpha(V_\mathrm{e}\sin\delta-v_i^k),\quad k=2,\end{cases}\tag{7}$$

where C_o is the obstacle avoidance control coefficient, which is set to 2, V_e the desired velocity, which is set to 10 m/s, v_i^k the velocity of the i^th UAV, and δ the desired obstacle avoidance course angle, which is equal to the inverse tangent between the i^th UAV and the nearest edge point of the nearest obstacle. Note that the field-of-view of a UAV is 180°, and that the obstacle perception distance is set to 120 m.

4. Consistent UAV speed control component u_nv:

$$u_\mathrm{nv}=C_\mathrm{nv}\sum_{j\in\{d_{ij}\le D_\mathrm{c}\}}\alpha(v_j^k-v_i^k),\tag{8}$$

where C_nv is the coefficient that keeps a consistent velocity with that of the neighbor, and is set to 0.2.

5. Expected speed control component u_ev:

$$u_\mathrm{ev}=C_\mathrm{ev}(0-v_i^k),\tag{9}$$

where C_ev is the coefficient that keeps a consistent velocity with the expected one, and is set to 8.

6. Vertical height control component u_eh:

$$u_\mathrm{eh}=C_\mathrm{eh}(h_\mathrm{e}-h_i),\tag{10}$$

where C_eh is the coefficient that keeps a consistent altitude with the expected one and is set to 20, and h_e is the desired altitude, which is set to 50 m.

2.3 Cost function design

To ensure the smooth and consistent passage of multiple UAVs in many obstacles, many control components need to be considered. In this study, two cost functions are designed according to the formation control effect and speed consistency (Qiu and Duan, 2020).

The first cost function is divided into two parts: (1) When there are obstacles within the detected range of the i^th UAV, the cost function represents the degree of passage through the obstacle zone, and its value is the projection of the horizontal position of the i^th UAV in the direction of the desired horizontal velocity. (2) When there is no obstacle within the detected range of the i^th UAV, the cost function represents the degree of consistency with the desired horizontal velocity. The first cost function is expressed as follows:

$$\mathrm{Cost}_1=\begin{cases}-\dfrac{(P_i^1,P_i^2)\cdot(v_\mathrm{e}^1,v_\mathrm{e}^2)}{V_\mathrm{e}},\quad \text{if } P_{i,\mathrm{obstacle}}\ne\varnothing,\\ \sum_{k=1}^{2}\left|v_\mathrm{e}-v_i^k\right|,\quad \text{otherwise},\end{cases}\tag{11}$$

where k=1, 2, v_e is the expected velocity, v_i the velocity of the ith UAV, and $P_{i,\text{obstacle}}$ the set of obstacles detected by the ith UAV.

The second cost function represents the performance of UAV flocking and the degree of consistency with neighbors' velocity, expressed as follows:

$$\text{Cost}_2 = \sum_{j\in\{d_{ij}\le D_c\}} l\left[(D_d - d_{ij}) + \sum_{k=1}^{2} |v_i^k - v_j^k|\right], \tag{12}$$

where l is the influence factor, and is set to 1.

In addition, two constraints need to be satisfied, which are the distance between a UAV and an obstacle and the distance among the UAVs within the safety threshold.

Therefore, the obstacle avoidance control strategy of multiple UAVs designed in this study can be transformed into a multi-objective optimization problem. Two cost functions are described above. The optimization parameter is the weight factor α, and the constraint conditions should be satisfied.

Note that for the variables in this study, the distance unit is m, the time unit is s, the velocity unit and the rate of change in altitude unit are both m/s, and the angle unit is rad. In addition, the constants of the flocking model are set according to Qiu and Duan (2020).

3 Multi-UAV obstacle avoidance control via MSLPIO

3.1 Social learning pigeon-inspired optimization

Cheng and Jin (2015) applied a social learning mechanism to PSO for the first time and obtained good results. The so-called social learning is the behavior of an individual to learn from its example. As an accessible example, you should learn from not only the students who are the first in school but also students who are better than you. The same principle applies to the biological groups. In this study, the social learning mechanism is introduced to MPIO, named MSLPIO. Detailed description of MSLPIO is given in this section.

Generally, swarm size is an important parameter for PIO and MPIO. It has no specific rules and is usually set at random. Therefore, we develop a method to determine the swarm size according to the search dimension, which is expressed as follows:

$$N = M + \text{floor}(D/5), \tag{13}$$

where N is the swarm size, M the base number, floor(D/5) the largest integer less than or equal to D/5, and D the search dimension. In this study, M is set to 50.

First, in the map and compass operation, pigeon positions and velocities are randomly generated and denoted as X_i=[x_{i1}, x_{i2}, …, x_{iD}] and V_i=[v_{i1}, v_{i2}, …, v_{iD}] (i=1, 2, …, N), respectively. New position X_i and velocity V_i at the next iteration are updated as follows:

$$\begin{cases} V_i^{\text{nc}} = V_i^{\text{nc}-1}\text{e}^{-R\cdot\text{nc}} + \text{rand}\cdot\text{c1}\cdot(X_{\text{model}} - X_i^{\text{nc}-1}), \\ X_i^{\text{nc}} = X_i^{\text{nc}-1} + V_i^{\text{nc}}, \end{cases} \tag{14}$$

where R is the map and compass factor, set between 0 and 1, nc the current number of iterations (when nc reaches the maximum iteration number of this stage, the map and compass operation ends), c1 the learning factor (c1=1−log(D/M)), and X_{model} the demonstrator position superior to the current pigeon. Each pigeon follows the superior one, and this is called the learning behavior. The schematic for selecting X_{model} is shown in Fig. 1.

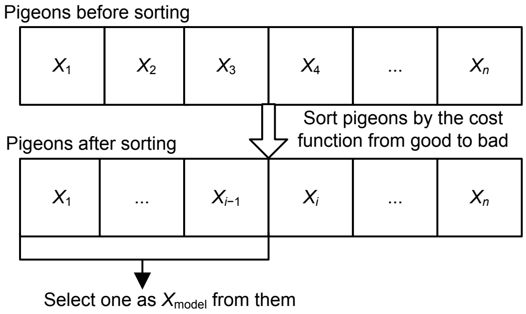
Pigeons before sorting
X1
X2
X3
X4
...
Xn
Sort pigeons by the cost function from good to bad
Pigeons after sorting
X1
...
Xi−1
Xi
...
Xn
Select one as Xmodel from them

Fig. 1 Social learning mechanism: how to select X_{model}

Second, in the landmark stage, pigeons from the center will be removed and other pigeons fly toward the center, which is called the social behavior. The update process is expressed as follows:

$$\begin{cases} X_{\text{center}}^{\text{nc}-1} = \sum_{i=1}^{N^{\text{nc}-1}} X_i^{\text{nc}-1} \Big/ N^{\text{nc}-1}, \\ N^{\text{nc}} = N^{\text{nc}-1} - N_{\text{removed}}, \\ X_i^{\text{nc}} = X_i^{\text{nc}-1} + \text{rand}\cdot\text{c2}\cdot(X_{\text{center}}^{\text{nc}-1} - X_i^{\text{nc}-1}), \end{cases} \tag{15}$$

where c2 is the social influence factor (c2=$\alpha(D/M)$, where α=0.5 is called the social coefficient) and N_{removed} the number of the pigeons removed in each iteration. When nc reaches the maximum iteration number, the landmark operator will stop.

3.2 Multi-objective social learning pigeon-inspired optimization (MSLPIO)

For a multi-objective optimization problem, it needs to balance multiple cost functions and select the best solution. The Pareto sorting scheme has been successfully used in many multi-objective optimization algorithms. It includes two steps: non-dominated sorting and crowded distance comparison. In this study, the Pareto sorting scheme is applied in MSLPIO.

1. Pareto sorting scheme

(1) Non-dominated sorting process

Position X_i of the i^{th} pigeon is considered superior to position X_j of the j^{th} pigeon, when both of the following conditions are satisfied:

$$\begin{cases}\text{Cost}_k(X_i)\leq\text{Cost}_k(X_j),\ k=1,2,\ldots,N,\\ \text{Cost}_{\bar{k}}(X_i)<\text{Cost}_{\bar{k}}(X_j),\ \text{at least one}\ \bar{k}\in\{1,2,\ldots,N\},\end{cases}\tag{16}$$

where Cost_k is the k^{th} cost function. Note that these conditions are for the minimization problems. For the maximization problem, a larger Cost_k should be selected.

Through a non-dominated sorting process, pigeons' positions will be divided into different sets and denoted as S_1^X, S_2^X, ..., S_m^X. The surface formed by solutions in the best non-dominated set S_1^X is known as the Pareto frontier.

(2) Crowded distance comparison

After the non-dominated sorting process, pigeons' positions in each set are arranged in descending order from large to small crowded distance.

The crowded distance of the i^{th} pigeon in set S_j^X is defined as follows:

$$\text{Dis}(X_i)=\frac{\text{Cost}_k(X_{i+1})-\text{Cost}_k(X_{i-1})}{\text{Cost}_k^{\max}-\text{Cost}_k^{\min}},\tag{17}$$

where $i\in\{2,3,\ldots,n_j^X-1\}$ and n_j^X is the number of pigeons in S_j^X. $\text{Cost}_k^{\max}$ and $\text{Cost}_k^{\min}$ are the maximum and minimum of the k^{th} cost function, respectively. Dis(X_1) and Dis($X_{n_j^X}$) are set to ∞. To ensure the diversity of solutions, a greater crowding distance is deemed to be better.

2. MSLPIO

To improve the flexibility of the algorithm, the map and compass operation and the landmark operation are combined. The specific process is expressed below:

$$\begin{cases}N^{\text{nc}}=N^{\text{nc}-1}-N_{\text{removed}},\\ V_i^{\text{nc}}=V_i^{\text{nc}-1}\text{e}^{-R\cdot\text{nc}}+\text{rand}\cdot\text{c1}\cdot(X_{\text{model}}-X_i^{\text{nc}-1})\\ \qquad+\text{rand}\cdot\text{c2}\cdot(X_{\text{center}}^{\text{nc}-1}-X_i^{\text{nc}-1}),\\ X_i^{\text{nc}}=X_i^{\text{nc}-1}+V_i^{\text{nc}},\end{cases}\tag{18}$$

where X_{model} and $X_{\text{center}}^{\text{nc}-1}$ are calculated from the data in Pareto frontier.

The pseudo code of MSLPIO is shown in Algorithm 1.

Algorithm 1 MSLPIO

```
/* Parameter initialization */
Set $M$=50, $D$=5, $\alpha$=0.5, $R$=0.3, $N_{\max}$=20, $N_{\text{removed}}$=2, $N$=$M$+floor($D$/5), c1=1−log($D/M$), c2=$\alpha(D/M)$, and the upper and lower bounds of the position and velocity
/* Pigeon initialization */
Initialize the positions and velocities of pigeons
Calculate the cost function
Obtain $X_{\text{model}}$ and $X_{\text{center}}$ by Pareto sorting
/* Main loop */
for nc=1 to $N_{\max}$ do
    Update positions by Eq. (18)
    Calculate the cost function
    Pareto sorting
    Calculate $X_{\text{center}}$ by Eq. (15)
    Store the Pareto frontier in $A$
    Pick one solution from $A$ as $X_{\text{model}}$
    nc=nc+1
    $N$=$N$−$N_{\text{removed}}$
end for
Output the Pareto frontier
```

To sum up, the complete steps of MSLPIO are as follows:

Step 1: Determine the swarm size N according to the search dimension D and set the maximum number of iterations ($N_{\max}$).

Step 2: Initialize the pigeons randomly with position X and velocity V. Set the upper and lower limits of position and velocity and take the limit values if they exceed the range.

Step 3: Calculate the cost function of each pigeon and perform the Pareto sorting scheme. Calculate $X_{\text{center}}^{\text{nc}-1}$ and add pigeons' positions in the Pareto frontier to archive A (A is the historical information base, used to store the Pareto frontier).

Step 4: Perform the Pareto sorting scheme again to pigeons' positions in A and keep the new Pareto frontier in A, which is denoted as $A=S_1^A$. X_{model} is any of A.

Step 5: Update velocity V and position X according to Eq. (18).

Step 6: Update iteration counter nc by nc=nc+1.

Step 7: Continue step 3 until nc reaches the maximum iteration number. Otherwise, output the optimal solution according to the Pareto frontier.

3.3 Total process of the proposed control strategy

According to the above UAV model and flocking control strategy, appropriate parameters are determined by MSLPIO, and finally the smooth passage of multiple UAVs in multiple obstacles is realized.

The multi-UAV obstacle avoidance control strategy via MSLPIO is shown in Algorithm 2.

Algorithm 2 The proposed control strategy

```
Parameter initialization
for $t$=1 to $T_{\max}$ do
    for $i$=1 to $N$ do
        Calculate control components by Eqs. (5)–(10)
        Obtain weight factor $\alpha$ by MSLPIO
        Obtain the final control variables and the control input
          of the $i^{\text{th}}$ UAV by Eqs. (2)–(4)
        Obtain the $i^{\text{th}}$ UAV state by Eq. (1)
        $i$=$i$+1
    end for
$t$=$t$+1
end for
Output all UAV states
```

4 Numerical simulation and comparison

In this section, we used MATLAB R2016a as the simulation tool and proved the proposed method by five UAVs flying among seven obstacles. The five UAVs were simulated by MATALB and generated by the UAV model in Section 2.1. The UAV model parameters were as follows: τ_V=1 s, τ_φ=0.75 s, τ_{a}=1/3 s, τ_{b}=3 s. The maximum and minimum horizontal velocities were 15 and 5 m/s, respectively. The maximum and minimum rates of change in altitude were 6 and −6 m/s, respectively. The obstacles were circles with different radii. The sampling time was 0.5 s and the maximum running time ($T_{\max}$) was 42 s.

Simulation results of the proposed method are shown in Fig. 2. In Fig. 2, the circles represent the obstacles, the triangles represent the UAVs, and the curves represent the flight paths of multiple UAVs. As can be seen in Fig. 2a, the obstacles were relatively dense, but multiple UAVs can form a tight formation and pass through the obstacles smoothly. UAVs did not pass through the obstacle areas above due to the designed control strategy. Velocity control components include the component consistent with the expected speed. Expected velocity was in a horizontal direction, so UAVs tended to be along the horizontal direction through the obstacles (Fig. 2a). It was proved that the designed control strategy in this study is feasible.

From Figs. 2b and 2c, in the obstacle areas, the speed fluctuated to a certain extent, and the yaw angle changed correspondingly. When multiple UAVs passed through the obstacle area, the velocity and yaw angle tended to be consistent very soon. From about 35 s, the velocity and yaw angle of all UAVs remained consistent and converged to the expected level, proving good convergence of the proposed MSLPIO. All the results demonstrated the effectiveness of the proposed method.

To highlight the advantages of MSLPIO based on the social learning mechanism, we made a comparison with the improved MPIO, and the simulation results are shown in Fig. 3. It can be seen from Fig. 3a that UAVs can pass through the obstacle areas; however, when the UAV flocking crossed the obstacle areas, several UAVs deviated from the course a little bit, and obvious bending occurred between 200 and 250 m. As can be seen in Fig. 3b, the speeds of all UAVs did not converge in the end, but fluctuated all the time, reflecting the inappropriateness of the optimization algorithm. In Fig. 3c, five UAVs' yaw angles eventually converged. The overall flocking control effect of MPIO was worse than that of the method proposed.

To further demonstrate the superiority of the proposed method, the NSGA-II algorithm proposed by Paul and Shill (2018) was simulated and analyzed, and the results are shown in Fig. 4. It can be seen that the UAVs can cross the obstacle areas well and the yaw angle can converge to the desired level, but the convergence speed was still poor. When crossing the first gap between two obstacles, the UAV group was a little crowded, and the formation of multiple UAVs gradually remained stable, but the speeds did not converge. This method is desirable in terms of the results of UAV flocking passing through obstacles, but it is inferior to the proposed method in terms of convergence.

In Table 1, the convergence time of velocities and yaw angles under the three algorithms is given. Considering the convergence of velocity, we can see that for MPIO and NSGA-II, the velocities did not converge to the desired one, and for MSLPIO, the velocities of the five UAVs converged to the desired one at 37 s. As for the convergence of yaw angles, among the three algorithms, MSLPIO converged the fastest, MPIO the second, and NSGA-II the slowest. The convergence rate of MSLPIO was 3.33% higher than that of MPIO and 5.88% higher than that of NSGA-II.

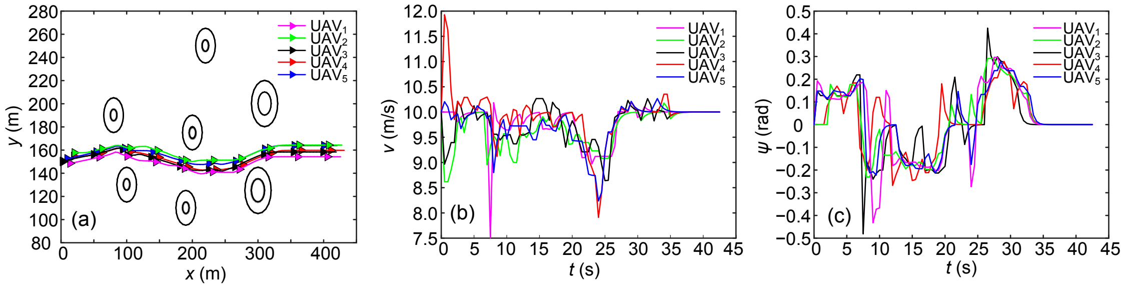

Fig. 2 Simulation results of MSLPIO: (a) obstacle avoidance process of UAV flocking; (b) velocity curves of UAVs; (c) yaw angle curves of UAVs

Circles represent the obstacles, triangles represent the UAVs, and curves represent the flight paths of multiple UAVs

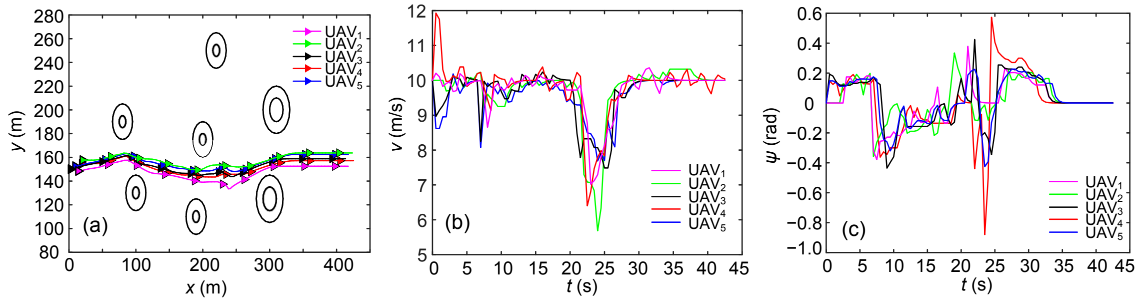

Fig. 3 Simulation results of MPIO: (a) obstacle avoidance process of UAV flocking; (b) velocity curves of UAVs; (c) yaw angle curves of UAVs

Circles represent the obstacles, triangles represent the UAVs, and curves represent the flight paths of multiple UAVs

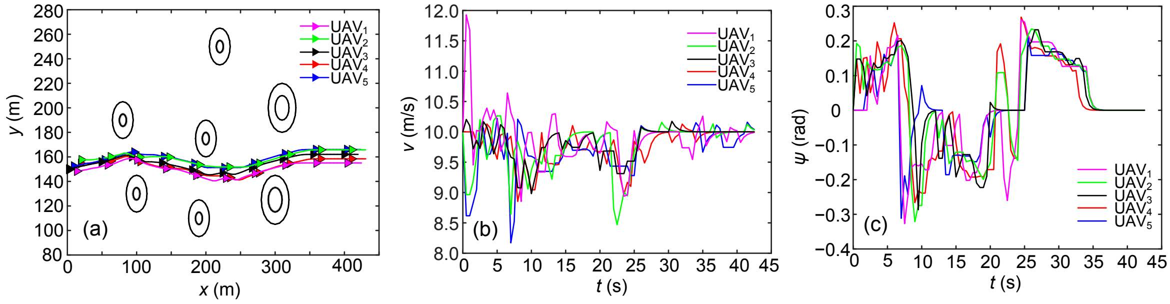

Fig. 4 Simulation results of NSGA-II: (a) obstacle avoidance process of UAV flocking; (b) velocity curves of UAVs; (c) yaw angle curves of UAVs

Circles represent the obstacles, triangles represent the UAVs, and curves represent the flight paths of multiple UAVs

Table 1 Statistical results of the three algorithms

Algorithm	Convergence time of velocities	Convergence time of yaw angles (s)
MSLPIO	37 s	33.75
MPIO	$>T_{\max}$	35.15
NSGA-II	$>T_{\max}$	36.22

$T_{\max}$: maximum running time

Through the above comparative analysis, although the UAV flocking optimized by MPIO and NSGA-II can pass through the obstacle areas, the consistency is poor, the speed cannot converge eventually, and it is difficult to meet the stability requirements. Finally, the validity and superiority of MSLPIO can be proved, and it has better convergence. Through the control parameter optimized by MSLPIO, multiple UAVs can smoothly pass through complex obstacles.

5 Conclusions

In this study, we improved MPIO using a social learning mechanism and successfully applied it to multi-UAV obstacle avoidance. The main conclusions are as follows: (1) The flocking control strategy does not need prior information about the environment, and the control framework is highly portable; (2) The convergence and consistency of MSLPIO are better than those of the comparable algorithms, and the UAV flocking can quickly converge to the expected level after crossing the obstacle areas.

Contributors

Hai-bin DUAN and Wan-ying RUAN designed the research. Wan-ying RUAN processed the data and drafted the manuscript. Hai-bin DUAN helped organize and check the manuscript. Wan-ying RUAN revised and finalized the paper.

Compliance with ethics guidelines

Wan-ying RUAN and Hai-bin DUAN declare that they have no conflict of interest.

References

Alonso-Mora J, Montijano E, Schwager M, et al., 2016. Distributed multi-robot formation control among obstacles: a geometric and optimization approach with consensus. Proc IEEE Int Conf on Robotics and Automation, p.5356-5363. https://doi.org/10.1109/icra.2016.7487747

Benjamin MR, Defilippo M, Robinette P, et al., 2019. Obstacle avoidance using multiobjective optimization and a dynamic obstacle manager. *IEEE J Ocean Eng*, 44(2):331-342. https://doi.org/10.1109/JOE.2019.2896504

Biro D, Sasaki T, Portugal SJ, 2016. Bringing a time-depth perspective to collective animal behaviour. *Trends Ecol Evol*, 31(7):550-562. https://doi.org/10.1016/j.tree.2016.03.018

Cheng R, Jin YC, 2015. A social learning particle swarm optimization algorithm for scalable optimization. *Inform Sci*, 291:43-60. https://doi.org/10.1016/j.ins.2014.08.039

Di B, Zhou R, Duan HB, 2015. Potential field based receding horizon motion planning for centrality-aware multiple UAV cooperative surveillance. *Aerosp Sci Technol*, 46:386-397. https://doi.org/10.1016/j.ast.2015.08.006

Duan HB, Qiao PX, 2014. Pigeon-inspired optimization: a new swarm intelligence optimizer for air robot path planning. *Int J Intell Comput Cybern*, 7(1):24-37. https://doi.org/10.1108/IJICC-02-2014-0005

Faisal M, Hedjar R, Al Sulaiman M, et al., 2013. Fuzzy logic navigation and obstacle avoidance by a mobile robot in an unknown dynamic environment. *Int J Adv Robot Syst*, 10(1):37. https://doi.org/10.5772/54427

Ferri G, Munafò A, LePage KD, 2018. An autonomous underwater vehicle data-driven control strategy for target tracking. *IEEE J Ocean Eng*, 43(2):323-343. https://doi.org/10.1109/JOE.2018.2797558

Floreano D, Wood RJ, 2015. Science, technology and the future of small autonomous drones. *Nature*, 521(7553): 460-466. https://doi.org/10.1038/nature14542

Forestiero A, 2017. Bio-inspired algorithm for outliers detection. *Multimed Tools Appl*, 76(24):25659-25677. https://doi.org/10.1007/s11042-017-4443-1

Guo X, Lu JQ, Alsaedi A, et al., 2018. Bipartite consensus for multi-agent systems with antagonistic interactions and communication delays. *Phys A*, 495:488-497. https://doi.org/10.1016/j.physa.2017.12.078

Ho HS, Do CS, 2017. Multi-agent based design of autonomous UAVs for both flocking and formation flight. *J Adv Korea Navig Technol*, 21(6):521-528. https://doi.org/10.12673/jant.2017.21.6.521

Kownacki C, Ambroziak L, 2017. Local and asymmetrical potential field approach to leader tracking problem in rigid formations of fixed-wing UAVs. *Aerosp Sci Technol*, 68:465-474. https://doi.org/10.1016/j.ast.2017.05.040

Luo QN, Duan HB, 2017. Distributed UAV flocking control based on homing pigeon hierarchical strategies. *Aerosp Sci Technol*, 70:257-264. https://doi.org/10.1016/j.ast.2017.08.010

Mohanty PK, Parhi DR, 2012. Path generation and obstacle avoidance of an autonomous mobile robot using intelligent hybrid controller. Proc 3rd Int Conf on Swarm, Evolutionary, and Memetic Computing, p.240-247. https://doi.org/10.1007/978-3-642-35380-2_29

Molinos EJ, Llamazares Á, Ocana M, 2019. Dynamic window based approaches for avoiding obstacles in moving.

Robot Auton Syst, 118:112-130.
https://doi.org/10.1016/j.robot.2019.05.003

Paul AK, Shill PC, 2018. New automatic fuzzy relational clustering algorithms using multi-objective NSGA-II. *Inform Sci*, 448-449:112-133.
https://doi.org/10.1016/j.ins.2018.03.025

Qiu HX, Duan HB, 2017a. Multiple UAV distributed close formation control based on in-flight leadership hierarchies of pigeon flocks. *Aerosp Sci Technol*, 70:471-486.
https://doi.org/10.1016/j.ast.2017.08.030

Qiu HX, Duan HB, 2017b. Pigeon interaction mode switch-based UAV distributed flocking control under obstacle environments. *ISA Trans*, 71:93-102.
https://doi.org/10.1016/j.isatra.2017.06.016

Qiu HX, Duan HB, 2020. A multi-objective pigeon-inspired optimization approach to UAV distributed flocking among obstacles. *Inform Sci*, 509:515-529.
https://doi.org/10.1016/j.ins.2018.06.061

Sun F, Turkoglu K, 2017. Distributed real-time non-linear receding horizon control methodology for multi-agent consensus problems. *Aerosp Sci Technol*, 63:82-90.
https://doi.org/10.1016/j.ast.2016.12.018

Wang J, Ahn IS, Lu YF, et al., 2017. A distributed estimation algorithm for collective behaviors in multiagent systems with applications to unicycle agents. *Int J Contr Autom Syst*, 15(6):2829-2839.
https://doi.org/10.1007/s12555-016-0015-9

Wu ST, 2013. Flight Control System (2nd Ed.). Beihang University Press, Beijing, China (in Chinese).

Yan MD, Zhu X, Zhang XX, et al., 2017. Consensus-based three-dimensional multi-UAV formation control strategy with high precision. *Front Inform Technol Electron Eng*, 18(7):968-977. https://doi.org/10.1631/FITEE.1600004

Zhang T, Li Q, Zhang CS, et al., 2017. Current trends in the development of intelligent unmanned autonomous systems. *Front Inform Technol Electron Eng*, 18(1):68-85.
https://doi.org/10.1631/FITEE.1601650

Zhao WW, Chu HR, Zhang MY, et al., 2019. Flocking control of fixed-wing UAVs with cooperative obstacle avoidance capability. *IEEE Access*, 7:17798-17808.
https://doi.org/10.1109/ACCESS.2019.2895643